LOW COMPLEXITY PRIMARY USER PROTECTION FOR COGNITIVE OFDM

Jorge F. Schmidt and Roberto López-Valcarce

Department of Signal Theory and Communications
University of Vigo, Spain

ABSTRACT

A novel active interference cancellation (AIC) scheme for primary user (PU) protection is presented for application to cognitive OFDM systems, in which out-of-band radiation spilling over the PU protected band is to be minimized. A set of cancellation subcarriers are modulated by appropriate linear combinations of the remaining data subcarriers. The combination coefficients are fixed and need not be changed on a symbol-by-symbol basis, in contrast with previous AIC approaches. Thus, the optimization can be carried out offline, drastically reducing the online implementation cost and power consumption. The proposed scheme is shown through simulations to outperform current AIC solutions at a lower computational cost.

1. INTRODUCTION

Orthogonal frequency division multiplexing (OFDM) has been widely adopted as the modulation technique for many broadband wireless communication systems because of its high spectrum efficiency and robustness against multipath fading. Further, its natural bandwidth partitioning makes it a particularly well suited modulation scheme for cognitive systems, where the transmit signal needs to be adjusted according to the available transmission spectrum. Nevertheless, the high out-of-band radiation (OBR) characteristic of OFDM remains a limiting factor for its application to cognitive systems, since it results in high interference for primary users (PUs) lying within the secondary user (SU) OFDM band.

In recent years, considerable attention has been given to this problem, and several solutions have been reported. The use of multiple choice sequences and constellation expansion techniques were proposed in [1] and [2] respectively. Both techniques require the transmission of side information to the receiver and thus increase the system overhead. On the other hand, active interference cancellation (AIC) oriented schemes [3]-[7] and precoding techniques [8]-[12] do not require side information at the receiver and are shown to have good OBR reduction performance. Precoding schemes naturally lead to low complexity implementations at the transmitter; however, the receiver needs to be aware of this fact and implement appropriate decoding of the received data. On the other hand, AIC schemes dedicate a subset of cancellation subcarriers in order to reduce OBR, without altering the data subcarriers. This operation is completely transparent to the receiver, which just needs to discard cancellation subcarriers, and thus a main advantage of AIC is its straightforward implementation in current systems.

In AIC schemes, the cancellation subcarriers are modulated by some function (usually a linear combination) of the symbols transmitted in the data subcarriers. Most solutions in the literature need to recompute the weights of the cancellation subcarriers at each OFDM symbol, making online computational cost a main concern [4]. This problem is exacerbated by the need to impose additional constraints in the optimization problem in order to keep the power allocated to cancellation subcarriers at bay, as in the constrained Least Squares (LS) approach of [3]. Reduced-complexity LS formulations were applied in [6] and [7], but the resulting power allocated to cancellation subcarriers is not kept under control. In contrast, a low-complexity implementation is derived in [5] by imposing individual power constraints on each cancellation subcarrier instead of an overall power constraint; however, this multiple constraint approach degrades significantly PU protection performance.

In this context, the main contribution of this paper is to derive a low complexity AIC scheme, without sacrificing PU protection performance. Different to reported AIC schemes, where optimization is performed over a discrete set of frequencies, the proposed approach is based on the direct minimization of the radiated power spilling over the PU protected band, computed as the integral of the power spectral density (PSD) over such band. This approach results in an AIC solution independent of the particular transmitted symbol, thus having a small online computational cost, since the cancellation weights can be computed offline. It is shown that the proposed formulation outperforms the schemes that use a set of discrete frequencies within the band, and does away with the problem of deciding these specific frequencies.

The remainder of this paper is organized as follows. The

Work supported by the Spanish Government, ERDF funds (TEC2010-21245-C02-02/TCM DYNACS, CONSOLIDER-INGENIO 2010 CSD2008-00010 COMONSENS), the Galician Regional Government (CN 2012/260 AtlantTIC), and the Instituto de Investigaciones en Ingeniería Eléctrica (IIIE)-Consejo Nacional de Investigaciones Científicas y Técnicas (CONICET), Universidad Nacional del Sur, Argentina.

signal model is presented in Sec. 2. In Sec. 3 the proposed AIC structure is defined, and the interference minimization over the PU band is derived. A performance evaluation to verify the effectiveness of the proposed approach is given in Sec. 4. Finally, conclusions are drawn in Sec. 5.

2. SIGNAL MODEL

A cognitive SU OFDM transmission with N subcarriers and power equally distributed among data subcarriers is considered. Focus is made on the case where a narrowband PU lies within the considered SU transmission bandwidth. It is assumed that the band $\mathcal{B}$ corresponding to the PU can be fitted within N_P contiguous SU subcarriers. SU subcarriers are allocated as follows: N_P subcarriers (aligned with band $\mathcal{B}$) plus N_C subcarriers (usually taking $N_C/2$ at each side of band $\mathcal{B}$) are reserved for the OBR reduction task[1]. The remaining $N_D = N - N_P - N_C$ subcarriers are unaffected and used for data transmission.

Based on this subcarrier allocation, an $N \times N_D$ matrix $\boldsymbol{S}$ is defined, containing the N_D columns of of the $N \times N$ identity matrix $\boldsymbol{I}_N$ corresponding to the data subcarriers. Analogously, we define the $N \times (N_P + N_C)$ matrix $\boldsymbol{T}$ containing the columns on $\boldsymbol{I}_N$ corresponding to the reserved subcarriers. Using these definitions, the $N \times 1$ vector modulating the SU subcarriers for a given OFDM symbol can be written as

$$\boldsymbol{x} = [\begin{array}{cccc} x_0 & x_1 & \cdots & x_{N-1} \end{array}]^T = \alpha \boldsymbol{S}\boldsymbol{d} + \boldsymbol{T}\boldsymbol{c}, \quad (1)$$

where $\boldsymbol{d}$ is the $N_D \times 1$ data vector, and $\boldsymbol{c}$ is a $(N_P + N_C) \times 1$ vector containing the cancellation coefficients to be modulated on the reserved subcarriers. The scaling factor α, with $0 < \alpha \leq 1$, is a user-selected parameter that allows to allocate the available transmit power between the data and cancellation subcarriers, as will be seen in Sec. 3.

To keep the presentation simple, conventional cyclic-prefix based OFDM is considered, in which a rectangular pulse shape is employed. Let Δ_f be the subcarrier spacing, and $T = (N + N_{\text{cp}})T_{\text{s}} = MT_{\text{s}}$ the OFDM symbol duration, with $T_{\text{s}} = 1/(N\Delta_f)$ and $M = N + N_{\text{cp}}$ the length of the cyclic-prefix extended symbol, measured in samples. The spectrum corresponding to the k-th subcarrier, windowed over one OFDM symbol, is given for $k = 0, 1, \ldots, N-1$ by

$$\phi_k(f) = M e^{-j\pi f \frac{M}{N} k} \operatorname{sinc}_M \left[\frac{1}{N} \left(\frac{f}{\Delta_f} - k \right) \right] \mathcal{G}(f), \quad (2)$$

where $\operatorname{sinc}_M[\cdot]$ stands for the periodic or aliased sinc function [13] and $\mathcal{G}(f)$ represents the frequency response of the interpolation filter used, assumed to be a perfect brickwall filter. Using (2), the SU spectrum can be expressed as

$$X(f) = \sum_{k=0}^{N-1} x_k \phi_k(f) = \boldsymbol{x}^T \boldsymbol{\phi}(f), \quad (3)$$

where $\boldsymbol{\phi}(f) = [\begin{array}{cccc} \phi_0(f) & \phi_1(f) & \cdots & \phi_{N-1}(f) \end{array}]^T$. From (1) and (3), the PU protection problem amounts to choosing the cancellation coefficients $\boldsymbol{c}$ (subject to appropriate design constraints) such that the resulting spectrum $X(f)$, measured over band $\mathcal{B}$, is 'small' in some sense. In the next section we address this problem by considering the radiated power over $\mathcal{B}$ as objective function.

3. PSD BASED LOW COMPLEXITY AIC

3.1. Derivation

We consider generating the cancellation coefficients $\boldsymbol{c}$ as linear combinations of the data symbols, i.e.,

$$\boldsymbol{c} = \boldsymbol{\Theta}\boldsymbol{d}, \quad (4)$$

where the $(N_P + N_C) \times N_D$ weight matrix $\boldsymbol{\Theta}$ is the parameter to be optimized. Note that $\boldsymbol{\Theta}$ is *fixed* and does not change from one OFDM symbol to the next (as long as the band $\mathcal{B}$ to protect does not change). Therefore, it can be computed offline, and thus the online complexity of the AIC scheme boils down to the computation of the product in (4) for each OFDM symbol. Inserting (4) in (1) gives

$$\boldsymbol{x} = (\alpha\boldsymbol{S} + \boldsymbol{T}\boldsymbol{\Theta})\boldsymbol{d} = \boldsymbol{G}\boldsymbol{d}. \quad (5)$$

Since the operator $\boldsymbol{G} \triangleq \alpha\boldsymbol{S} + \boldsymbol{T}\boldsymbol{\Theta}$ is memoryless and static (time-invariant), the signal PSD can be approximated as

$$\begin{aligned} P_x(f) \approx E\left\{|X(f)|^2\right\} &= \boldsymbol{\phi}^H(f) E\{\boldsymbol{x}\boldsymbol{x}^H\} \boldsymbol{\phi}(f) \\ &= \boldsymbol{\phi}^H(f) \boldsymbol{G} E\{\boldsymbol{d}\boldsymbol{d}^H\} \boldsymbol{G}^H \boldsymbol{\phi}(f) \\ &= \operatorname{tr}\{\boldsymbol{G}^H \boldsymbol{\Phi}(f) \boldsymbol{G}\}, \end{aligned} \quad (6)$$

where we have assumed that the data are zero-mean i.i.d. with covariance $E\{\boldsymbol{d}\boldsymbol{d}^H\} = \boldsymbol{I}_{N_D}$, and we have also introduced the Hermitian matrix $\boldsymbol{\Phi}(f) \triangleq \boldsymbol{\phi}(f)\boldsymbol{\phi}^H(f)$.

The goal is to minimize the out-of-band radiation, under the constraint that the total transmit power is fixed whether $\boldsymbol{x} = \boldsymbol{S}\boldsymbol{d}$ or (5) is used, i.e.

$$\min_{\boldsymbol{\Theta}} \int_{\mathcal{B}} P_x(f) \mathrm{d}f \quad \text{s.t.} \int_{-\infty}^{\infty} P_x(f) \mathrm{d}f \leq P_{\max}. \quad (7)$$

Introducing the $N \times N$ matrices $\boldsymbol{\Phi}_{\mathcal{B}} \triangleq \int_{\mathcal{B}} \boldsymbol{\Phi}(f)\mathrm{d}f$ and $\boldsymbol{\Phi}_{\mathcal{T}} \triangleq \int_{-\infty}^{\infty} \boldsymbol{\Phi}(f)\mathrm{d}f$, (7) can be rewritten as

$$\begin{aligned} &\min_{\boldsymbol{\Theta}} \operatorname{tr}\{\boldsymbol{G}^H(\boldsymbol{\Theta}) \boldsymbol{\Phi}_{\mathcal{B}} \boldsymbol{G}(\boldsymbol{\Theta})\} \\ &\quad \text{s.t.} \quad \operatorname{tr}\{\boldsymbol{G}^H(\boldsymbol{\Theta}) \boldsymbol{\Phi}_{\mathcal{T}} \boldsymbol{G}(\boldsymbol{\Theta})\} \leq P_{\max}. \end{aligned} \quad (8)$$

Note that different to previously reported AIC schemes, the solution of (8), which concentrates most of the computational load, needs to be computed only once and that computation can be performed offline and stored. Since both $\boldsymbol{\Phi}_{\mathcal{B}}$ and $\boldsymbol{\Phi}_{\mathcal{T}}$ are Hermitian, one can resort to generalized singular

[1] While data transmission on subcarriers aligned with $\mathcal{B}$ is forbidden, these can still be modulated with nonzero coefficients to enhance OBR reduction.

value decomposition (gsvd) tools [14] in order to efficiently obtain the solution. Let $\boldsymbol{\theta}_i$ and $\boldsymbol{s}_i$, with $i = 1, \ldots, N_D$, be the columns of matrices $\boldsymbol{\Theta}$ and $\boldsymbol{S}$ respectively, and let

$$P_{d_{\mathcal{T}}} = \alpha^2 \operatorname{tr}\{\boldsymbol{S}^T \boldsymbol{\Phi}_{\mathcal{T}} \boldsymbol{S}\}, \;\; P_{d_{\mathcal{B}}} = \alpha^2 \operatorname{tr}\{\boldsymbol{S}^T \boldsymbol{\Phi}_{\mathcal{B}} \boldsymbol{S}\}, \quad (9)$$

be the contribution of the data subcarriers to the total power and to the power leaked over band $\mathcal{B}$, respectively. Then, Problem (8) can be written as

$$\begin{aligned} \min_{\{\boldsymbol{\theta}_i\}} \;\; & P_{d_{\mathcal{B}}} + \sum_{i=1}^{N_D} \left[\boldsymbol{\theta}_i^H \boldsymbol{A}^H \boldsymbol{A} \boldsymbol{\theta}_i + 2\alpha \Re\left\{\boldsymbol{\theta}_i^H \boldsymbol{A}^H \boldsymbol{p}_i\right\}\right] \\ \text{s.t.} \;\; & P_{d_{\mathcal{T}}} + \sum_{i=1}^{N_D} \left[\boldsymbol{\theta}_i^H \boldsymbol{B}^H \boldsymbol{B} \boldsymbol{\theta}_i + 2\alpha \Re\left\{\boldsymbol{\theta}_i^H \boldsymbol{B}^H \boldsymbol{q}_i\right\}\right] = P_{\text{max}}, \end{aligned} \quad (10)$$

where the matrices $\boldsymbol{A}$, $\boldsymbol{B}$ and the vectors $\boldsymbol{p}_i$, $\boldsymbol{q}_i$ are given by

$$\boldsymbol{A} = \boldsymbol{P}_A^H \boldsymbol{\Lambda}_A^{1/2} \boldsymbol{P}_A, \qquad \boldsymbol{p}_i = \boldsymbol{A}^{-1} \boldsymbol{T}^T \boldsymbol{\Phi}_{\mathcal{B}} \boldsymbol{s}_i, \quad (11)$$

$$\boldsymbol{B} = \boldsymbol{P}_B^H \boldsymbol{\Lambda}_B^{1/2} \boldsymbol{P}_B, \qquad \boldsymbol{q}_i = \boldsymbol{B}^{-1} \boldsymbol{T}^T \boldsymbol{\Phi}_{\mathcal{T}} \boldsymbol{s}_i, \quad (12)$$

with $\boldsymbol{P}_A$, $\boldsymbol{P}_B$ unitary matrices and $\boldsymbol{\Lambda}_A$, $\boldsymbol{\Lambda}_B$ diagonal matrices given by the eigendecompositions

$$\boldsymbol{T}^T \boldsymbol{\Phi}_{\mathcal{B}} \boldsymbol{T} = \boldsymbol{P}_A^H \boldsymbol{\Lambda}_A \boldsymbol{P}_A, \qquad \boldsymbol{T}^T \boldsymbol{\Phi}_{\mathcal{T}} \boldsymbol{T} = \boldsymbol{P}_B^H \boldsymbol{\Lambda}_B \boldsymbol{P}_B. \quad (13)$$

Consider now the gsvd of $\boldsymbol{A}$ and $\boldsymbol{B}$ [14], given by

$$\boldsymbol{A} = \boldsymbol{U} \boldsymbol{D}_A \boldsymbol{X}^{-1}, \qquad \boldsymbol{B} = \boldsymbol{V} \boldsymbol{D}_B \boldsymbol{X}^{-1}, \quad (14)$$

where $\boldsymbol{U}$, $\boldsymbol{V}$ are unitary, $\boldsymbol{X}$ is invertible, and $\boldsymbol{D}_A$, $\boldsymbol{D}_B$ are diagonal and positive semidefinite with $\boldsymbol{D}_A^2 + \boldsymbol{D}_B^2 = \boldsymbol{I}$. Following [14, Ch.12], the solution of (10) is given by

$$\boldsymbol{\theta}_i = -\alpha \boldsymbol{X} (\boldsymbol{D}_A^2 + \lambda \boldsymbol{D}_B^2)^{-1} (\boldsymbol{D}_A \boldsymbol{U}^H \boldsymbol{p}_i + \lambda \boldsymbol{D}_B \boldsymbol{V}^H \boldsymbol{q}_i), \quad (15)$$

for $i = 1, \ldots, N_D$, where λ is the unique Lagrange multiplier such that the solution (15) attains the power constraint. Although the value of λ has to be found numerically, the function over which to search for it is monotonically decreasing from $\lambda = 0$ (no power constraint), such that the value of λ satisfying the power constraint can be easily found [14].

3.2. PSD-AIC computational cost

Disregarding matrices $\boldsymbol{S}$ and $\boldsymbol{T}$ that just map cancellation coefficients and data symbols to subcarriers, the online computational cost for PSD-AIC is given by the calculation of (4) which requires only $2 \times (N_C + N_P) \times N_D$ operations.

It is clear that most of the computational effort, i.e. the optimization of $\boldsymbol{\Theta}$, is performed offline. This is not the case in previous solutions [3],[5]. Further, the online computational cost of AIC schemes found in the literature depends directly on the frequency resolution, that is, the number of frequency points in band $\mathcal{B}$ considered in the optimization. In our approach, although the integration step required in order to compute $\boldsymbol{\Phi}_{\mathcal{B}}$ and $\boldsymbol{\Phi}_{\mathcal{T}}$ has to be carried out numerically in general, which also involves some frequency resolution, this does not affect online complexity. As will be shown in Sec. 4, the proposed approach leads to improved PU protection performance thanks to the better spectral resolution available.

	$N_C = 6$	$N_C = 8$	$N_C = 10$
Full load	-17.8	-17.8	-17.8
Null subcarriers	-20.6	-21.1	-21.6
PSD-AIC $\alpha^2 = 0.99$	-28.1	-31.9	-36.8
PSD-AIC $\alpha^2 = 0.98$	-30.2	-36.2	-40.3
PSD-AIC $\alpha^2 = 0.97$	-32.0	-38.6	-41.8
PSD-AIC $\alpha^2 = 0.96$	-33.6	-39.9	-42.5
PSD-AIC $\alpha^2 = 0.95$	-34.9	-40.7	-43.1

Table 1. Mean notch depth over protected band $\mathcal{B}$ (dB)

4. PERFORMANCE EVALUATION

The performance of the proposed scheme, termed PSD-AIC, is evaluated in this section. Comparison is made against the baseline scenarios of a fully loaded system (which only turns off the N_P subcarriers aligned with $\mathcal{B}$) and a system employing N_C null subcarriers to reduce OBR. Further, comparison against the cancellation subcarrier schemes of [3] and [5], which have comparable features is also provided.

To get a realistic evaluation, OFDM parameters are chosen based on current standards specifications [15, 16]. We consider an SU OFDM system consisting of $N = 1024$ subcarriers, together with a narrowband PU lying within the SU spectrum and with a bandwidth equivalent to $N_P = 20$ subcarriers. Data symbols to be modulated on the data subcarriers are i.i.d. and chosen from a $16-$QAM constellation. A 5% CP is used, equivalent to 48 samples. Transmission power is shared between data and cancellation subcarriers through parameter α (see (5)), which is varied from $\alpha^2 = 0.95$ to $\alpha^2 = 0.99$ such that the power spent on the cancellation subcarriers is a small fraction of the available power.

PU protection performance of the proposed PSD-AIC is considered in the results shown in Table 1. Specifically, it is shown that for $N_C = 8$ and $\alpha^2 = 0.97$ the notch depth is increased 17.5 dB and more than 20 dB with respect to the null subcarriers and the fully loaded cases respectively, demonstrating the effectiveness of the proposed scheme.

Figs. 1 and 2 show the behavior of the proposed scheme as the power on the cancellation subcarriers is increased while keeping N_C fixed, and as N_C is varied for a fixed cancellation power respectively. It can be noted how an increasing cancellation power improves the notch depth over the protected band, while it also increases the PSD peak values at the band edges due to the N_C cancellation subcarriers. It can also be noted that increasing N_C for a fixed α also improves the notch depth while reducing the PSD peak values as cancellation power is distributed among more subcarriers.

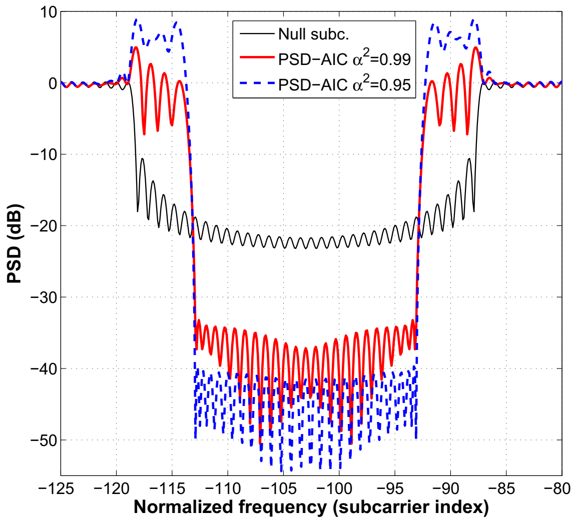

Fig. 1. PSDs of proposed PSD-AIC for $N_C = 10$ cancellation subcarriers and increasing cancellation power.

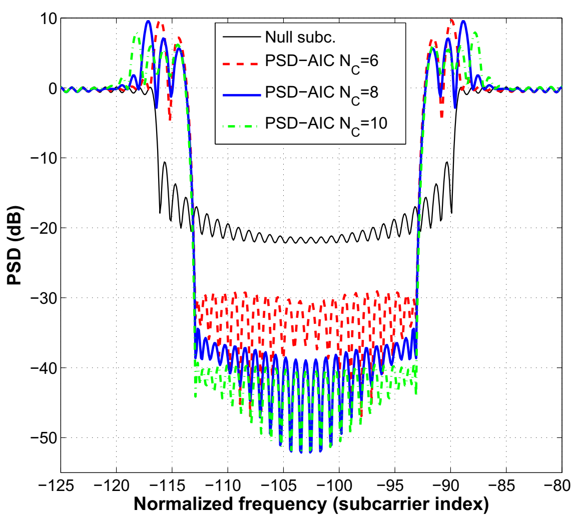

Fig. 2. PSDs of proposed PSD-AIC for $\alpha^2 = 0.97$ and different amounts of cancellation subcarriers.

Figs. 3 and 4 compare the proposed active cancellation scheme with those from [3] and [5], referred to in the sequel as AIC and SR-AIC respectively. Both AIC and SR-AIC are based on the minimization of the SU spectrum over a discrete set of frequencies within $\mathcal{B}$. In particular, $M = 10$ samples per sidelobe are taken for the computations presented, as suggested by the authors to keep online computational load reasonable (the cancellation coefficients are computed *online* for each OFDM symbol in both schemes). On the other hand, the matrices $\mathbf{\Phi}_{\mathcal{B}}$ and $\mathbf{\Phi}_{\mathcal{T}}$ featuring in the proposed method are evaluated numerically using a frequency resolution of 100 samples per sidelobe. Regarding the power constraint on the cancellation subcarriers, while AIC is designed under a power constraint equivalent to the one employed in this paper, this is not the case for SR-AIC. In SR-AIC an *individual* power constraint for each cancellation subcarrier is used. In the results presented here, these constraints are set all equal.

	Online complexity	Example
PSD-AIC	$2(N_C + N_P)N_D$	$55,776$
AIC [3]	$\mathcal{O}(2NM+$ $1/2N_C^2M + 2/3N_C^3)$ $+2M(N_C+N_P)N_D$	$> 578,789$
SR-AIC [5]	$2NM + 2M(N_C+N_P)N_D$	$578,240$

Table 2. Online computational cost for compared AIC schemes. The last column indicates the approximate load for the parameters of Figs. 3 and 4.

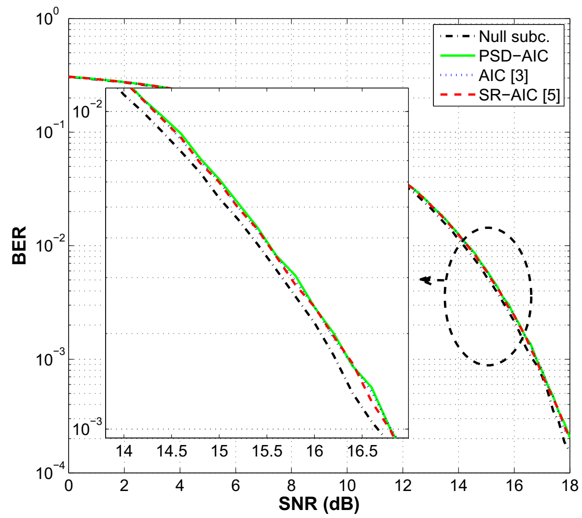

Fig. 3. BER performance for PSD-AIC, AIC [3] and SR-AIC [5] for $N_C = 8$ and $\alpha^2 = 0.97$. Results are averaged over 500 OFDM symbols.

Fig. 3 shows the bit error rate (BER) performance vs. SNR. It can be seen that all compared AIC schemes exhibit a fixed SNR loss due to the power allocated to the cancellation subcarriers. As long as α^2 is close to 1, as will be the case in realistic situations, this SNR loss is not significant.

Although performance in terms of BER is similar for all compared AIC schemes, this is not the case for PU protection performance, as shown in Fig. 4. Normalized power spectra are plotted to this end using the same parameters as in Fig. 3. The main difference in performance between SR-AIC

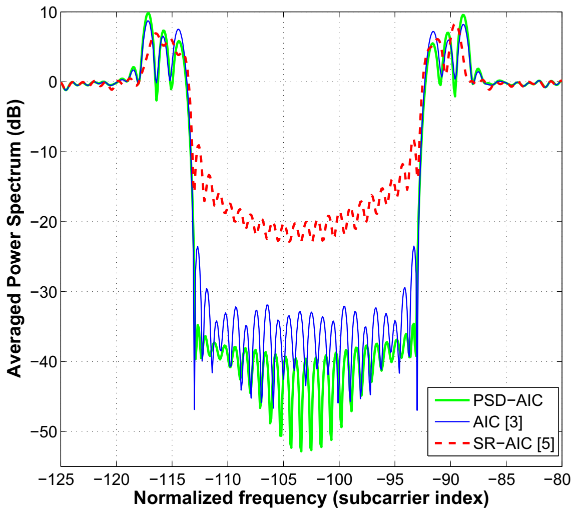

Fig. 4. Averaged power spectrum for PSD-AIC, AIC [3] and SR-AIC [5] for $N_C = 8$ and $\alpha^2 = 0.97$. Results are averaged over 500 OFDM symbols.

and both PSD-AIC and AIC arises for the different constraint used. The power constraints used in SR-AIC are more restrictive on the cancellation coefficients, leading to a significant performance loss in terms of OBR reduction. On the other hand, performance of AIC and proposed PSD-AIC is comparable, although favoring the proposed scheme. In this case the power constraints in the two optimization problems are equivalent; the better performance of PSD-AIC is obtained from the finer frequency resolution, which is obtained without compromising online computational cost.

Table 2 further emphasizes the complexity savings of the proposed structure. The online complexity for the three compared schemes is shown and the impact of M (samples per sidelobe for the set of discrete frequencies) becomes evident. The large complexity savings of PSD-AIC come from the fact that its online computational cost is independent of the frequency resolution used. The computational cost for proposed PSD-AIC is less than 10% of that of AIC and SR-AIC resulting in computational savings of more than 90%.

5. CONCLUSIONS

A novel AIC structure was proposed for PU protection in cognitive OFDM systems, based on the definition of the cancellation subcarriers as linear combination of the data subcarriers. A low-complexity scheme for PU protection was derived from this structure, exploiting the fact that the structure definition enables most of the computational load to be performed offline. It was shown that the proposed scheme outperforms current AIC solutions in terms of PU protection at a much lower computational cost.

6. REFERENCES

[1] I. Cosovic and V. Janardhanam, "Sidelobe suppression in OFDM systems," in *MCSS*, 2005, pp. 473 –482.

[2] S. Pagadarai, R. Rajbanshi, A. Wyglinski, and G. Minden, "Sidelobe suppression for OFDM-based cognitive radios using constellation expansion," in *IEEE Wireless Comm. and Networking Conf. (WCNC)*, Apr. 2008, pp. 888 –893.

[3] S. Brandes, I. Cosovic, and M. Schnell, "Reduction of out-of-band radiation in OFDM systems by insertion of cancellation carriers," *IEEE Comm. Letters*, vol. 10, no. 6, pp. 420 –422, June 2006.

[4] H. Yamaguchi, "Active interference cancellation technique for MB-OFDM cognitive radio," in *34th European Microwave Conf.*, vol. 2, Oct. 2004, pp. 1105 –1108.

[5] S.-G. Huang and C.-H. Hwang, "Improvement of active interference cancellation: avoidance technique for OFDM cognitive radio," *IEEE Trans. on Wireless Comm.*, vol. 8, no. 12, pp. 5928 –5937, Dec. 2009.

[6] D. Qu, Z. Wang, and T. Jiang, "Extended active interference cancellation for sidelobe suppression in cognitive radio OFDM systems with cyclic prefix," *IEEE Trans. on Vehicular Technology*, vol. 59, no. 4, pp. 1689 –1695, May 2010.

[7] A. Batra, S. Lingam, and J. Balakrishnan, "Multi-band OFDM: a cognitive radio for UWB," in *IEEE Int. Symp. on Circuits and Systems (ISCAS)*, May 2006, pp. 4 pp. –4097.

[8] J. Zhang, X. Huang, A. Cantoni, and Y. Guo, "Sidelobe suppression with orthogonal projection for multicarrier systems," *IEEE Trans. on Comm.*, vol. 60, no. 2, pp. 589 –599, Feb. 2012.

[9] J. Van De Beek, "Sculpting the multicarrier spectrum: a novel projection precoder," *IEEE Comm. Letters*, vol. 13, no. 12, pp. 881 –883, Dec. 2009.

[10] H.-M. Chen, W.-C. Chen, and C.-D. Chung, "Spectrally precoded OFDM and OFDMA with cyclic prefix and unconstrained guard ratios," *IEEE Trans. on Wireless Comm.*, vol. 10, no. 5, pp. 1416 –1427, May 2011.

[11] M. Ma, X. Huang, B. Jiao, and Y. Guo, "Optimal orthogonal precoding for power leakage suppression in DFT-based systems," *IEEE Trans. on Communications*, vol. 59, no. 3, pp. 844 –853, Mar. 2011.

[12] R. Xu and M. Chen, "A precoding scheme for DFT-based OFDM to suppress sidelobes," *IEEE Comm. Letters*, vol. 13, no. 10, pp. 776 –778, Oct. 2009.

[13] T. van Waterschoot, V. Le Nir, J. Duplicy, and M. Moonen, "Analytical expressions for the power spectral density of CP-OFDM and ZP-OFDM signals," *IEEE Signal Proc. Letters*, vol. 17, no. 4, pp. 371 –374, Apr. 2010.

[14] G. H. Golub and C. F. van Van Loan, *Matrix Computations*, 3rd ed. The Johns Hopkins University Press, Oct. 1996.

[15] 3GPP, "Physical layer aspects for evolved UTRA," 3GPP technical report, TR 25.814, Ver. 7.1.0, 2009.

[16] WiMax, "IEEE standard for local and metropolitan area networks part 16: Air interface for fixed and mobile broadband wireless access systems," IEEE Std 802.16e, 2006.